Original Research Article

Ultra-Wideband Metamaterial-based Rectangular Microstrip Antenna for Sub-6 GHz 5G and other Microwave Applications

ABSTRACT

This paper presents a novel design of an ultra-wideband metamaterial-based rectangular microstrip antenna for sub-6 GHz 5G and other microwave applications. The proposed antenna consist of a rectangular microstrip patch, two metamaterial unit cells, Flame Resistant (FR-4) substrate ($\varepsilon_r = 4.2$) and partial ground plane. The metamaterial unit cell comprises complementary split ring resonator (CSRR) with double negative characteristics (negative permeability and negative permittivity) as well as negative refractive index (NRI). The NRI medium enhanced the bandwidth and radiation efficiency of the antenna by reducing the surface waves and mutual coupling. The antenna operates over frequency range of 3.4009 to 11.721 GHz and 2.869 to 3.211 GHz, covering the sub-6 GHz 5G bands and other microwave applications such as Wi-Fi, WiMAX, and WLAN. Also, the proposed antenna had optimized dimensions of $2.857\ \lambda_0 \times 0.292\ \lambda_0 \times 0.0186\ \lambda_0$ and exhibited good impedance matching, omnidirectional radiation pattern, and stable gain across the operating band. From simulation results, a combined bandwidth of 8.66 GHz was achieved which shows good agreement with outlined objective. The proposed antenna is suitable for sub-6 GHz 5G and other microwave applications that require ultra-wideband performance and low-profile design.

Keywords: Metamaterial, ultra-wideband, antenna, microwave, sub-6 GHz

1. INTRODUCTION

Contemporarily, the noticeable rise in the number of wireless communication devices is a proof of the relentless technological innovations that has become recognisable with the modern age [1]. Among these innovations, [2] stated that mobile phones are adjudged to have evolved the most because they now evidently possess similar data processing power as full-fledged computers and incorporate modems for different standards of wireless communication including the fifth generation (5G) of mobile communication reported to have significantly improved data throughput in comparison to earlier generations. These wireless communication standards according [3], are in most cases deployed on different frequency bands (majorly around the sub-6 GHz bands) thus reemphasizing the need for suitable multiband antennas with inherent characteristics such as low-profile, lightweight and being conformable to mounting surface. Microstrip antenna (MSA) possesses these characteristics which makes them the predominant choice for miniature antennas [4]. However, MSAs are limited by their narrow bandwidth (usually between $1-5\%$ fractional bandwidth) that requires additional means to achieve wide bandwidth [5].

Split Ring Resonator (SRR) structures due to their ability to alter antenna electromagnetic properties have been reported by several authors as one of the mechanisms used to enhance antenna performance [1], [6], [7]. Alteration of antenna properties by SRR is aided by their dual electromagnetic behaviour (either as single negative or double negative material). Generally, structures such as SRR are classified as metamaterials; metamaterials as defined by [8], is an artificial material with in-built capability to exhibit electromagnetic properties not readily found in naturally occurring materials such as, negative refractive index and artificial magnetism.

Some previously published works related to the study were reviewed. Yongfeng in [9] proposed an integrated ultrawideband/narrowband rectangular dielectric resonator antenna (DRA) for cognitive radio with two symmetrical short-circuited strips for improved isolation between two ports. Compact UWB dielectric resonator antenna with dual-band-rejection characteristics for WiMAX/WLAN bands was reported by [10] from which the authors achieved bandwidth enhancement by embedding stub and slot of various lengths on a DRA. Also, [11] presented a compact bi-cone dielectric resonator antenna for ultra-wideband applications. The layout of these DRA antennas however placed an intrinsic limit on their extent of application. Thanuj et al. [12] presented obround-shaped metamaterial based compact planar antenna for UWB and 5G applications; the antenna was designed on Rogers RT Duroid 5880 substrate with a thickness of 0.43 mm which achieved a fractional bandwidth of approximately 50% with good radiation efficiency. Metamaterial inspired multiband antenna for 5G sub-6 GHz New Radio (NR) frequency bands and wireless applications was proposed by [13] with dimensions of $36 \times 22 \times 1.6\,mm^3$ on flame resistant (FR-4) substrate which achieved a fractional impedance bandwidth of 47.20%.

This paper presents a unique design of an ultra-wideband (UWB) metamaterial-based rectangular microstrip antenna for sub-6GHz 5G and other microwave applications. The proposed antenna consists of a rectangular patch with a partial ground plane and two metamaterial unit cells integrated adjacent to the feedline of the patch and located on the same side of the substrate. The metamaterial unit cell is composed of SRR which provides negative permittivity characteristics. The design process of the proposed metamaterial-based patch is described in Section 2 with different development steps including that of unit cell, antenna performance characteristics is presented in Section 3, where detailed parametric study and surface current distribution of the proposed antenna are discussed using simulated results. The paper is concluded in section 5, which is followed by the list of references used.

2. METHODOLOGY

In this section, the design procedures for single band microstrip antenna at sub-6 GHz 5G frequency band of 3.5 GHz followed by the considerations for the design of unit cell metamaterial and finally, the integration of the patch with the metamaterial are presented.

2.1 Single Band Patch Antenna Design

A single band microstrip antenna with centre frequency of 3.5 GHz is first designed using transmission line model equations obtained from [5], [14], [15]. The rectangular patch structure acts as a resonator; thus, the length and width of the patch are typically selected in such a way that $L_P < W_P < 2L_P$ for efficient and enhanced radiation. The design equations used for the rectangular microstrip patch are itemized as follows:

i) The width (W_P) of the microstrip patch is computed from Equation 1.

$$W_P = \frac{C}{2f_r\sqrt{\frac{(\varepsilon_r+1)}{2}}} \quad (1)$$

ii) The effective dielectric constant (ε_{reff}) is obtained from Equation 2.

$$\varepsilon_{reff} = \frac{\varepsilon_r+1}{2} + \frac{\varepsilon_r-1}{2}\left[1+12\left(\frac{h}{W_P}\right)\right]^{-1/2} \quad (2)$$

iii) The effective length L_{eff} of the patch is calculated from Equation 3.

$$L_{eff} = \frac{c}{2f_r\sqrt{\varepsilon_{reff}}} \quad (3)$$

iv) The length extension (ΔL) is deducted from the length of the patch (L_P) with actual length of the patch unchanged (in most cases). The length extension is considered due to fringing field as seen in Equation 4.

$$\Delta L = 0.412h\,\frac{[\varepsilon_{reff}+0.3]\left[\frac{W}{h}+0.264\right]}{[\varepsilon_{reff}-0.258]\left[\frac{W}{h}+0.813\right]} \quad (4)$$

v) Calculation of actual length of patch (L_P) is done using Equation 5.

$$L_{eff} = L_P + 2\Delta \quad (5)$$

$$L_P = L_{eff} - 2\Delta L \quad (6)$$

vi) Calculation of the ground plane dimensions (Lg and Wg): A major assumption adopted by the transmission line model is the use of infinite ground planes for simplified analysis. However, it is essential to have a finite ground plane for practical contemplations. For both finite and infinite ground planes, the size of the ground plane must be greater than the patch dimensions by approximately six times the substrate thickness (h) all around the patch periphery [5]. Hence, for this design, the ground plane dimensions are calculated thus:

$$Lg = L_P + 6h \quad (7)$$

$$Wg = W_P + 6h \quad (8)$$

vii) Determination of the patch thickness (t): The metallic patch is selected to be very thin such that t << λ_0.

Inset-fed technique was used for the feedline to the patch, and the design equations were adopted from [16], [17]. Table containing computed dimensions of the 3.5 GHz single band patch antenna is presented in Table 1 while the schematic diagram and single band rectangular microstrip antenna modelled in CST Studio are given in Fig. 1.

Table 1. Computed dimensions of 3.5 GHz single band edge-fed RMSA

Design Parameter	Values
Patch dimensions:	
Length (L_p)	20.45 mm
Width (W_p)	26.58 mm
Dielectric constant (ε_r)	4.2
Substrate height (h)	1.60 mm
Patch thickness (t)	0.35 mm
Ground plane dimensions:	
Length of ground plane (L_g)	30.05 mm
Width of ground plane (W_g)	36.18 mm
Feed line dimensions:	
Width of 50 Ω transmission line (W_f)	3.10 mm
Length of 50 Ω transmission line (L_f)	4.80 mm
Input edge impedance of the patch (R_{in})	185.19 Ω
Characteristic impedance of the feed line (Z_0)	50 Ω
Inset fed gap (g)	1.80 mm
Inset fed distance, (y_o)	7.55 mm

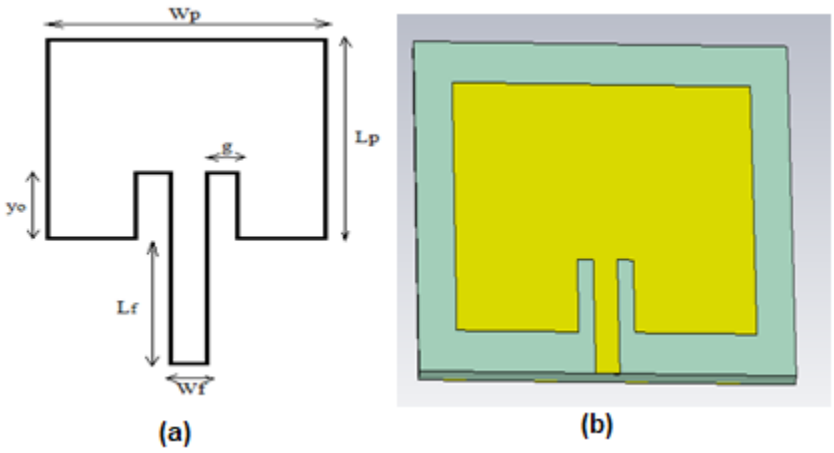

Fig. 1. Designed antenna (a) schematic diagram (b) 3.5 GHz patch

2.2 Unit cell metamaterial

Depending on the structure and size of a unit cell, different corresponding values of permittivity (ε), permeability (μ) and resonant frequencies (f_r) can be obtained. For each unit cell geometry, the dimensions can be adjusted to satisfy designed conditions at resonance frequency (f_r) [7]. According to [3], unit cell size is approximately one-tenth of the operating wavelength (λ_{air}), that is, the retrieval of effective parameters from reflection and transmission data depends on the fact that unit-cell dimension should be smaller than the operating wavelength in the media. Hence, taking the one-tenth of the wavelength of the reference antenna (3.5 GHz antenna) to be the external length (L_m) of the metamaterial (MTM), the external ring length of the MTM is computed to be 8.57 mm. The MTM shape of choice for this study is the split ring resonator (SRR) selected mainly for ease of design and analysis. Based on the report put forward by [18], every dimension of the complementary

square SRR (see Fig. 2(a)) is duly accounted for with a simplified relationship between the components typified in the equivalent circuit presented in Fig. 2(b) such as capacitance (C), inductance (L) and $\mathrm{f_r}$ given in Equation 9.

$$L_m = \frac{85.71}{10} = 8.57\ mm$$

Other parameters considered in SRR design are – the ring's outer radius, a, thickness, c, height, h, and the width of gap, g. The square SRR is modelled by an inductance, L; the gap in the ring corresponds to capacitance, C_{gap} which is modelled as a parallel plate capacitor; the charges on the surface are the surface capacitance, $C_{surface}$. According to [19], with magnetic field applied along the z-axis, an electromotive force appears around the SRR making the structure behave in similar fashion like an L-C network having resonant frequency $(\mathrm{f_r})$ expressed in Equation 9.

$$\mathrm{f_r} = \frac{1}{2\pi\sqrt{LC}} \tag{9}$$

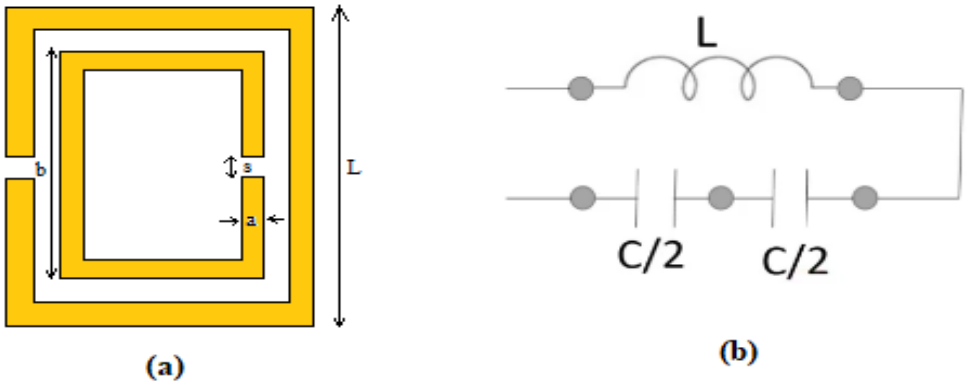

Fig. 2. Metamaterial (a) Geometry of unit cell SRR (b) Equivalent circuit representation of unit cell SRR [18]

In the same vein, the inductance can be approximated by that of a closed ring [19].

$$L = \mu_0 a_m \left(ln \frac{8a_m}{h+c} - 0.5 \right) \tag{10}$$

Note: $a_m = a + \frac{w}{2}$

$$C_{gap} = \varepsilon_0 \left(\frac{ch}{g} + \frac{2\pi h}{ln\frac{2.4h}{c}} \right) \tag{11}$$

$$C_{surface} = \frac{2\varepsilon_0 h}{\pi} \ln \frac{4a}{g} \tag{12}$$

$$\frac{1}{C} = \frac{1}{C_{gap}} + \frac{1}{C_{surface}} \tag{13}$$

where μ_0 is the permeability of free space, a is the outer radius of ring and a_m is the mean radius of the ring.

The dimensions of the metamaterial unit cell are given in Table 2.

Table 2. Dimensions of SRR

Parameter	Value (mm)
L_m	8.57
s	1
a	1
b	6

2.3 Patch Antenna with Metamaterial

The single band patch antenna designed in Section 2.1 and two SRR structure designed in Section 2.2 were integrated with FR-4 substrate while partial ground plane was introduced to offset current flow and consequently alter the impedance bandwidth by shifting the antenna resonance frequency. This resulted in patch antenna size reduction at the same centre frequency. The front and back view of the proposed metamaterial-based patch antenna are presented in Fig. 3 while the optimized patch dimensions are tabulated in Table 3.

Table 3. Dimensions of proposed antenna

Design Parameter	Values
Patch and feedline dimensions:	
Length (L_p)	13 mm
Width (W_p)	14 mm
Dielectric constant (ε_r)	4.2
Substrate height (h)	1.60 mm
Patch thickness (t)	0.35 mm
Width of 50 Ω transmission line (W_f)	4 mm
Length of 50 Ω transmission line (L_f)	14 mm
Ground plane dimensions:	
Length of ground plane (L_g)	25 mm
Width of ground plane (W_g)	30 mm

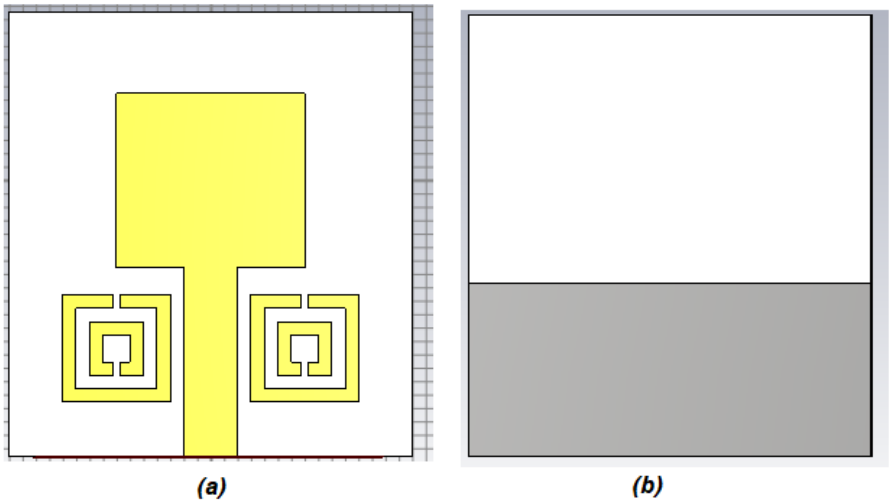

Fig. 3. Proposed MTM-based patch antenna (a) front-view (b) back-view

3. RESULTS AND DISCUSSION

The return loss plot of the single band patch antenna designed at 3.5 GHz showed a minimum return loss value of -27.16 dB at 3.52 GHz as depicted in Fig. 4. The bandwidth achieved by the single band patch was approximately 70 MHz which represents 2% fractional bandwidth of the 3.5 GHz band. Also, the s-parameter (S_{11} and S_{21}) of the unit cell metamaterial is illustrated in Fig. 5 from which minimum return loss values of -22.49 and -60.47 dB at 13.69 GHz are observed. Real and imaginary plots of permittivity and permeability of the unit cell metamaterial is presented in Fig. 6 and Fig. 7.

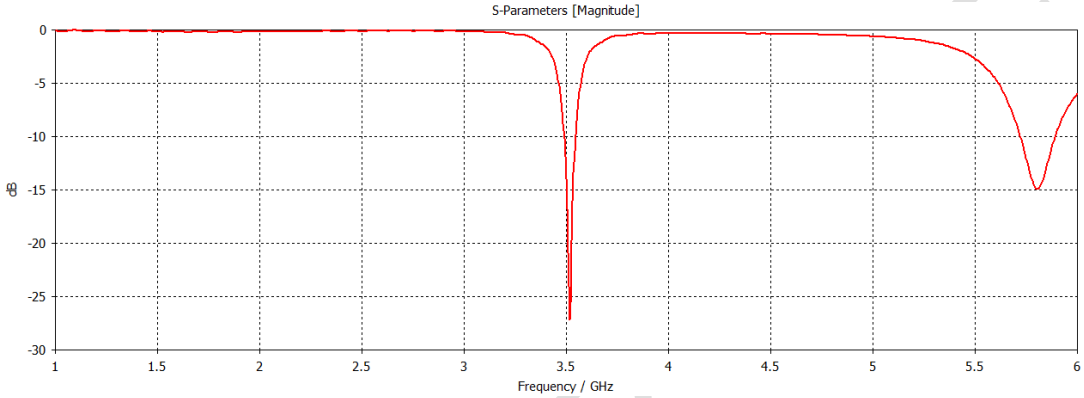

Fig. 4. Return loss of 3.5 GHz RMSA

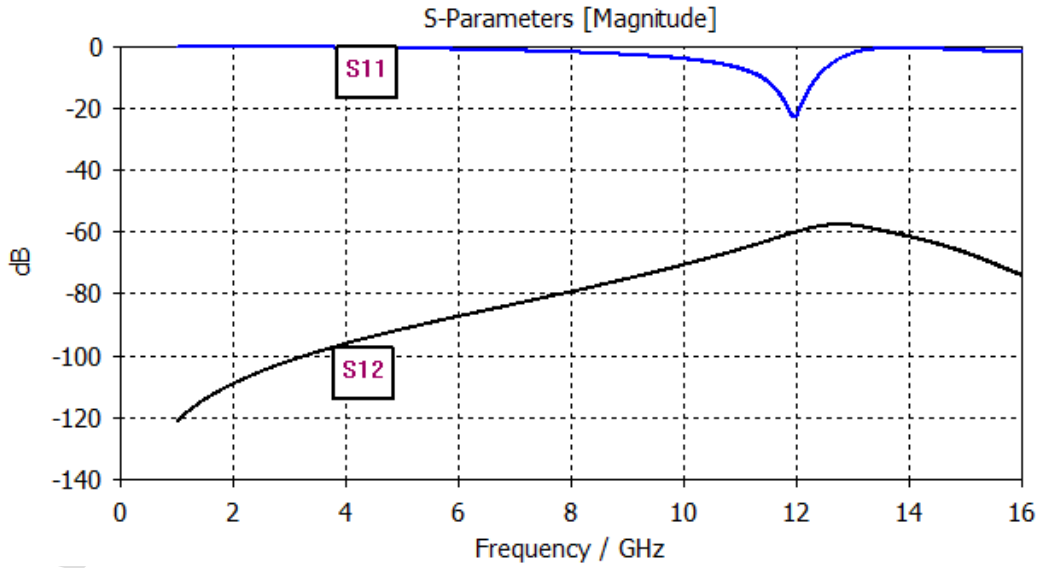

Fig. 5. S_{11} and S_{12} plot of SRR structure

From Fig. 6 and Fig. 7, negative permittivity and permeability values at resonance frequency of 11.95 GHz are observed which affirms that the SRR designed in Section 2.2 is a double negative (DU) metamaterial. Signal to the units are mainly by induction both from the

antenna feedline and also the patch element. Fig. 8 gives the return loss plot of the proposed metamaterial-based antenna from which a combined bandwidth of 8.66 GHz was achieved over two distinct range of frequencies (3.4009 GHz – 11.721 GHz and 2.869 GHz – 3.211 GHz). Based on the definition of ultrawide-band (UWB) antenna given by [20], the return loss characteristics depicted in Fig. 8 shows that the proposed antenna fits the profile.

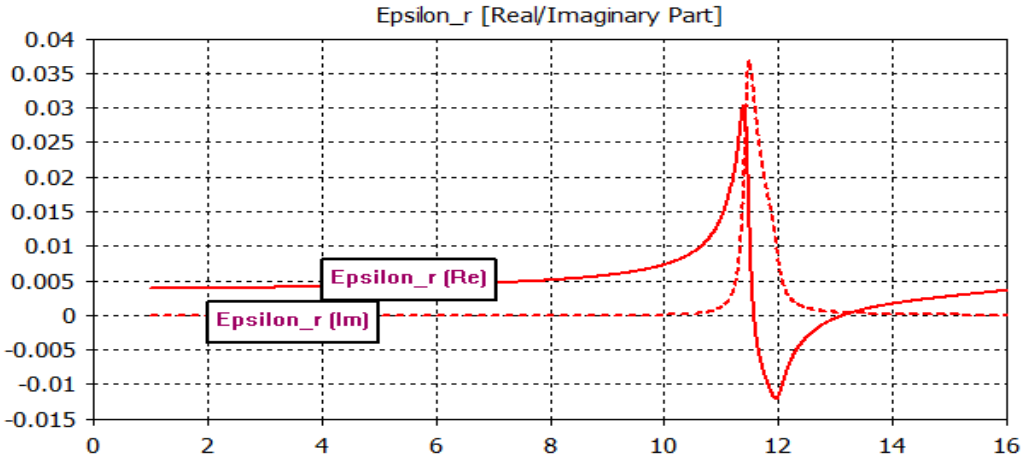

Fig. 6. Real and Imaginary values of permittivity

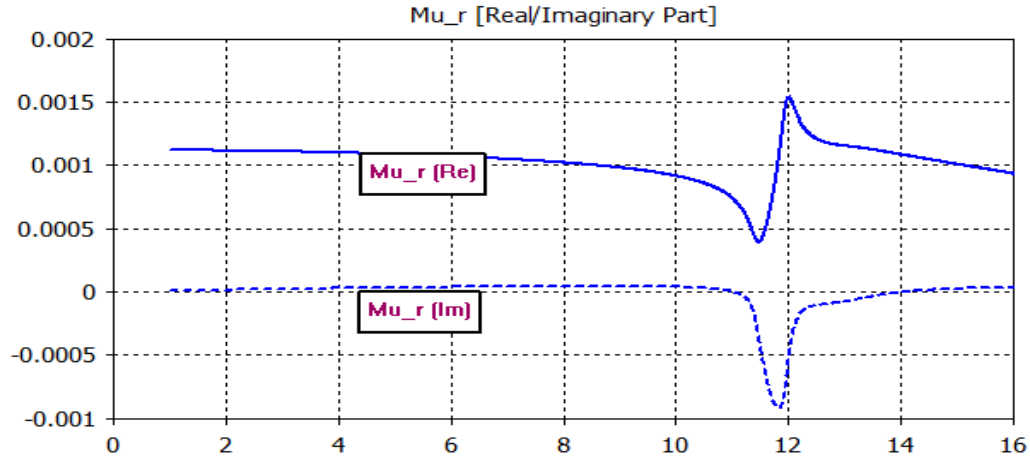

Fig. 7. Real and Imaginary values of permeability

Also, from performance analysis of simulated results, radiation efficiency of 78% and gain of 2.17 dBi was achieved by the proposed antenna are presented in Fig. 9 and Fig. 10. This signifies that substantial amount of the power fed to the antenna is equally radiated.

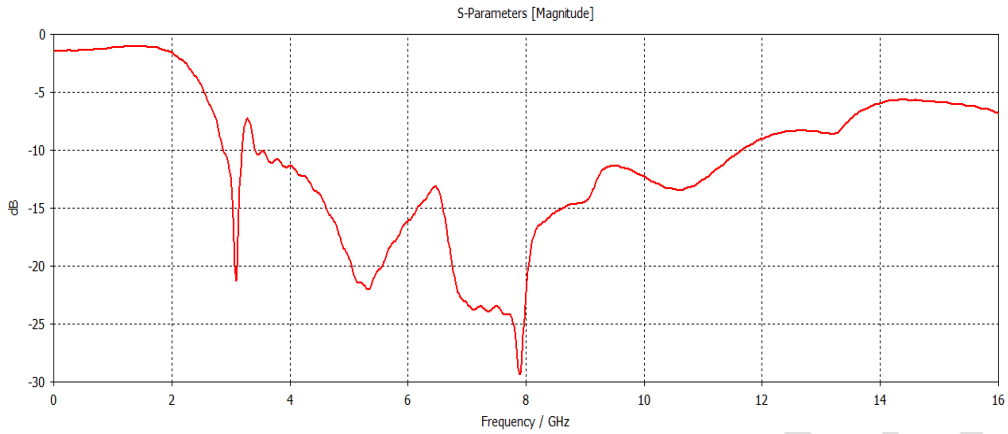

Fig. 8. Return loss of proposed metamaterial antenna

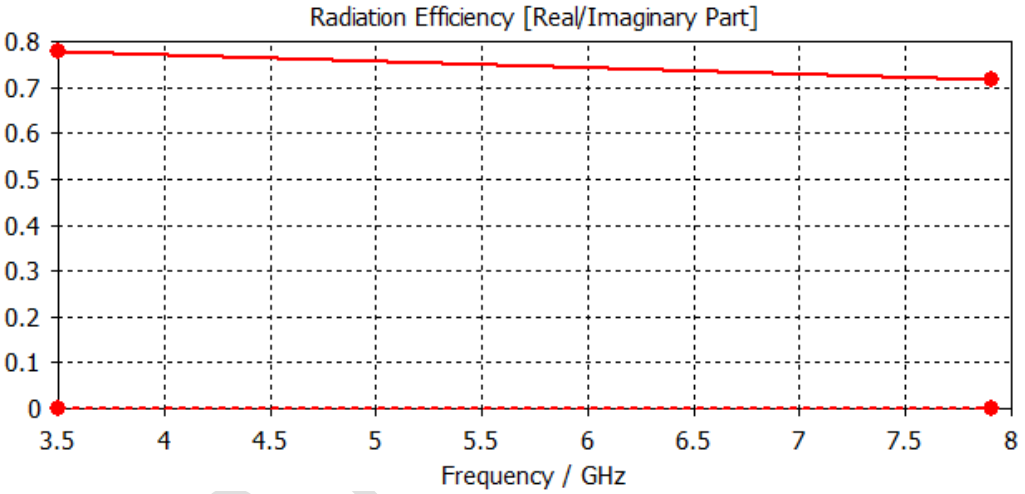

Fig. 9. Radiation efficiency of proposed metamaterial antenna

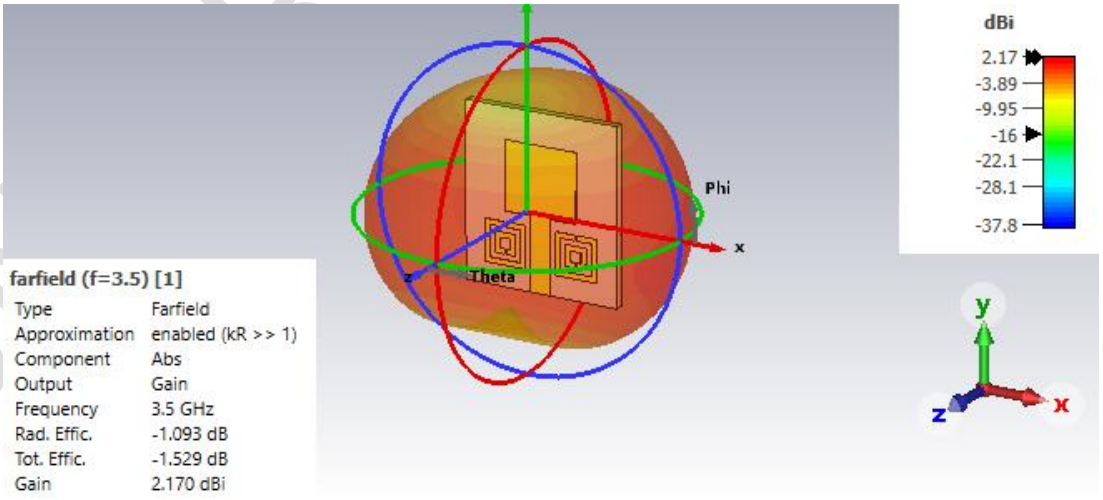

Fig. 10. 3-D plot of proposed metamaterial antenna gain

The antenna presented in this study showed broadside and bidirectional radiation pattern for E- and H-plane at 3.5 GHz which is at variance with the traditional directive pattern of microstrip antennas as illustrated in Fig. 11.

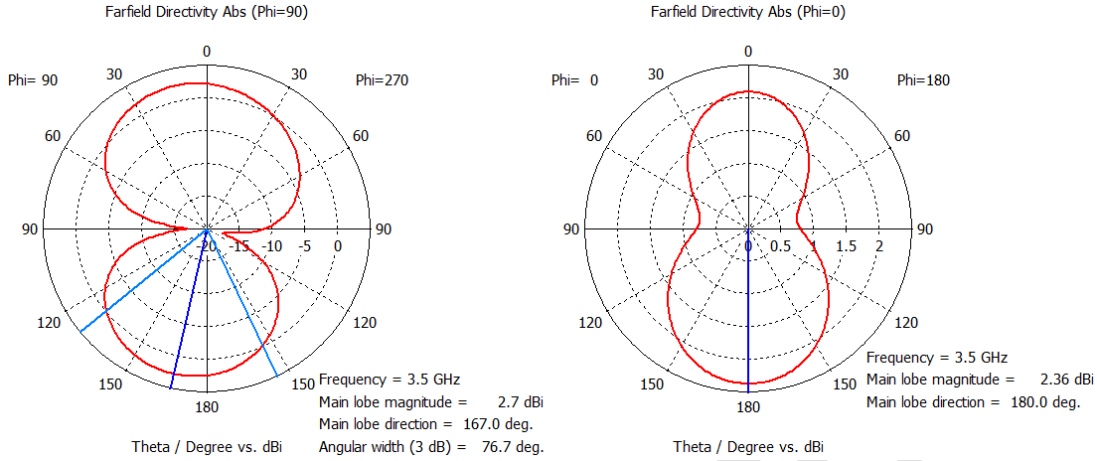

Fig. 11. H-plane and E-plane of proposed antenna

Brief comparison of the antenna proposed in this study with some related literatures is presented in Table 4. The antenna reported in this study occupied lesser footprint $(30 \times 25 \times 1.6\, mm^3)$ compared to those reported by [20] and [21] which where $40 \times 24.5 \times 1.6\, mm^3$ and $30 \times 30 \times 1.6\, mm^3$.

Table 4: Brief comparison of the antenna with related literatures

Journal	Antenna Dimension (mm^3)	Bandwidth (dB)	Peak Gain (dB)	Rad. Eff. (%)
[20]	$40 \times 24.5 \times 1.6$	8.30	6.52	92
[21]	$30 \times 30 \times 1.6$	7.20	7.90	80
[22]	$10 \times 10 \times 0.7$ $10 \times 15 \times 0.7$	28.50	6.2	70
[23]	$19.6 \times 17 \times 1.6$	3.70	6.2	-
[24]-	$20 \times 20 \times 1.6$	2.15	4.7	-
Proposed work	$30 \times 25 \times 1.6$	8.66	2.71	78

4. CONCLUSION

In this paper, metamaterial-based patch antenna has been designed for sub-6 GHz 5G and other microwave applications. The proposed antenna comprises an edge-fed rectangular patch, two metamaterial unit cells at the top and a partial ground plane at the bottom of FR-4 substrate. Simulation results showed that a combined bandwidth of 8.66 GHz was achieved by the proposed antenna representing 50% fractional bandwidth. Also, distinct radiation pattern from typical microstrip antennas was observed for E- and H-pane at 3.5 GHz. The extended bandwidth coverage as well as the reduced footprint qualifies the antenna proposed for integration in portable devices for 5G and other microwave applications.

REFERENCES

1 Al-Bawri SS, Islam MT, Islam MS, Singh MJ and Alsaif H. Massive metamaterial system-loaded MIMO antenna array for 5G base stations. *Sci. Rep.* 2022;12(1): 1–16

2 Hasan MM, Faruque MRI and Islam MT. Dual band metamaterial antenna for LTE/bluetooth/WiMAX system. *Sci. Rep.* 2018;8(1): 1–17.

3 Abdullah N, Bhardwaj G and Sunita. Design of squared shape SRR metamaterial by using rectangular microstrip patch antenna at 2.85 GHz. *SPIN 2017*. 2017:196–200.

4 Kumari R and Kumar M. Frequency reconfigurable multi-band inverted T-slot antenna for wireless application. In *Proceedings of the 2014 International Conference on Advances in Computing, Communications and Informatics, ICACCI 2014*. 2014:696–699.

5 Balanis CA. *Antenna Theory, Analysis and Design.*, 3rd ed. New Jersey: John Wiley & Sons, 2016.

6 Antipov SP, Wanming L, Power JG and Spentzouris LK. Left-handed metamaterials studies and their application to accelerator physics *Proc. IEEE Part. Accel. Conf.* 2005: 458–460.

7 Rani SS and Naik KK. Design and Analysis of Complimentary Split Ring Resonator with Slot on Retangular Patch Antenna for Wireless Applications. *Int. J. Recent Technol. Eng. 2019;*7(6):50–53.

8 Bose S, Ramaraj M, Raghavan S and Kumar S. Mathematical Modeling, Equivalent Circuit Analysis and Genetic Algorithm Optimization of an N-sided Regular Polygon Split Ring Resonator (NRPSRR). *Procedia Technol.* 2012;6:763–770.

9 Wang Y, Wang N, Denidni TA, Zeng Q and Wei G. Integrated ultrawideband/narrowband rectangular dielectric resonator antenna for cognitive radio. *IEEE Antennas Wirel. Propag. Lett.* 2014;13: 694–697.

10 Abedian M, Rahim SKA, Danesh S, Hakimi S, Cheong LY and Jamaluddin MH. Novel design of compact UWB dielectric resonator antenna with dual-band-rejection characteristics for WiMAX/WLAN bands. *IEEE Antennas Wirel. Propag. Lett.* 2015; 14: 245–248.

11 Sankaranarayanan D, Venkatakiran D, and Mukherjee B. Compact bi-cone dielectric resonator antenna for ultra-wideband applications–a novel geometry explored. *Electromagnetics. 2017;*37(7):471–481.

12 Thanuj D, Saravana KN, Gnanamoorthi NB and Stanislaus RJ. Metamaterial based compact planar antenna for UWB and 5G applications. *Proc. - 2nd Int. Conf. Micro-Electronics Telecommun. Eng. ICMETE. 2018*;33–35.

13 Saraswat RK. Design and Analysis of Metamaterial Inspired Multiband Antenna for 5G Sub-Six GHz NR Frequency Bands and wireless applications. 2022;1–29.

14 Kumar G and Ray KP. *Broadband microstrip antennas*. MA, USA: Artech House. 2003.

15 Huang Y and Boyle K. *Antennas From Theory to Practice*, 1st ed. West Sussex, United Kingdom: John Wiley & Sons, 2008.

16 Saturday JC. Udofia KM and Obot AB. Compact Rectangular Slot Patch Antenna for

Dual Frequency Operation Using Inset Feed Technique. *Int. J. Inf. Commun. Sci.* 2017;1(3):47–53.

17 Nsidibe-Emmanuel NC., Udofia, KM and Obot, AB. Dual Band Rectangular Microstrip Antenna Array for Wireless Communication. *European Journal of Basic and Applied Sci.* 2019;6(1):37–44.

18 Rajni and Marwaha A. An accurate approach of mathematical modeling of SRR and SR for metamaterials. *J. Eng. Sci. Technol. Rev.* 2016;9(6):82–86.

19 Vani HR. Paramesha and Goutham MA. Design and Analysis Of Square Split Ring Resonator Metamaterial. *Int. J. Adv. Res. Eng. Technol.* 2018;9(6):196–201.

20 Nejdi IH, Bri S, Marzouk M, Ahmad S, Rhazi Y, Ait LM, Sheikh YA, Ghaffar A, Hussein M. UWB Circular Fractal Antenna with High Gain for Telecommunication Applications. Sensors, 2023;3(8):4172.

21 Iftikhar UD, Sadiq U, Syeda IN, Raza U, Shakir U, Esraa MA and Mohammad A. Improvement in the Gain of UWB Antenna for GPR Applications by Using Frequency-Selective Surface. International Journal of Antennas and Propagation, 2022, Article ID 2002552, 12 pages, 2022, 1-12.

22 Alhawari ARH, Almawgani AHM, Hindi AT, Alghamdi H and Saeidi T. Metamaterial-based wearable flexible elliptical UWB antenna for WBAN and breast imaging applications. AIP Advances, 2021;11,1-12.

23 Sourav R, Krishna LB, and Ujjal C. Beam Focusing Compact Wideband Antenna Loaded with Mu-Negative Metamaterial for Wireless LAN Application. Progress In Electromagnetics Research. 2018;83, 33-44.

24 Shashank K, Sravan BV, Aluru N, Saadh AWM, Poonkuzhali R, Kumar OP, Ali T and Pai MMM. A compact wideband antenna with detailed time domain analysis for wireless applications, Ain Shams Engineering Journal. 2020;11(4): 1131-1138.